K-shell x-ray production in Ge, Rb, Y, Zr, and Ag by ^{14}N ion impact*

J. Tricomi, J. L. Duggan, and F. D. McDaniel
North Texas State University,† Denton, Texas 76203

P. D. Miller
Oak Ridge National Laboratory, Oak Ridge, Tennessee 37830

R. P. Chaturvedi and R. M. Wheeler
State University of New York College, Cortland, New York 13045

J. Lin
Tennessee Technological University, Cookeville, Tennessee 38501

K. A. Kuenhold
University of Tulsa, Tulsa, Oklahoma 74104

L. A. Rayburn
University of Texas at Arlington, Arlington, Texas 76019

S. J. Cipolla
Creighton University, Omaha, Nebraska 68178
(Received 18 December 1975; revised manuscript received 6 December 1976)

K-shell x-ray production cross sections for Ge, Rb, Y, Zr, and Ag have been measured for incident ^{14}N ions in the energy range 7–35 MeV. Ionization cross sections are calculated from atomic K-shell fluorescence yields and compared with the plane-wave Born approximation (PWBA) theory modified to include the effects of increased target binding energy, Coulomb deflection of the incident projectile, target polarization, and relativistic K-shell electron velocities. Experiment and theory are in very good agreement and indicate that the PWBA with modifications is quite appropriate for the projectile-target combinations and energy range for the measurements presented in this report.

I. INTRODUCTION

The plane-wave Born approximation (PWBA) theory for K-shell ionization, as modified by Basbas, Brandt, and Laubert[1] to include the effects of increased electron binding energy when ionization takes place inside the K-shell electron orbitals and Coulomb deflection of the incident projectile, has been found by many experimenters to be in reasonable agreement with K-shell ionization cross sections inferred from measured x-ray production cross sections. This has been shown for a variety of target atoms and incident heavy ions with velocities from 0.1 to 1 times the average K-shell electron velocity. Further modification to the PWBA is indicated for ionization by the faster projectiles,[2,3] and Basbas and co-workers[4] have developed modifications to the PWBA which include the effects of target-electron wave-function polarization by projectiles whose velocities are comparable to those of the K-shell electrons. In addition, corrections to account for relativistic electron velocities in heavy targets for which the atomic number $Z > 30$ have been found to improve agreement between experiment and theory at low projectile velocities.[3,5–7]

The object of the present investigation was experimental determination and theoretical description of the K-shell x-ray production cross sections of $_{32}Ge$, $_{37}Rb$, $_{39}Y$, $_{40}Zr$, and $_{47}Ag$ for incident ^{14}N ions in the energy range 7 to 35 MeV. For these energies, ion velocities were in the range of from 0.15 to 0.3 times the target K-shell electron velocities, and the modified PWBA formalism of Basbas *et al.*[1,4] should adequately describe the ionization process.

Another objective of this experimental work was to examine $K\alpha/K\beta$ ratios and shifts of the characteristic x-ray energies of the targets. This information has been used to indicate the degree of multiple ionization of L and/or M shells at the time of K-shell vacancy production.

II. EXPERIMENTAL PROCEDURE

^{14}N ions in charge states from 3^+ to 5^+ and energies from 7 to 35 MeV were provided by the EN Tandem Van de Graaff accelerator at the Oak Ridge National Laboratory. The ion beam was collimated to a diameter of 2 mm on target by two tantalum apertures. A carbon aperture approximately 3 cm in front of the target helped to minimize beam spraying of the aluminum target frames.

Thin transmission targets, vacuum deposited upon 15 to 50 $\mu g/cm^2$ carbon backings, were mounted at 45° to the incident ^{14}N ion beam direction. The approximate target thicknesses were: $_{32}Ge$, 40 $\mu g/cm^2$; $_{37}Rb$, 40 $\mu g/cm^2$; $_{39}Y$, 60 $\mu g/cm^2$; $_{40}Zr$, 10 $\mu g/cm^2$; and $_{47}Ag$, 70 $\mu g/cm^2$. A 6-mm-diam Si(Li) detector with a 0.00076-cm Be entrance window was positioned within the evacuated scattering chamber approximately 5 cm from the target and at 90° with respect to the incident beam direction. In order to reduce the count rate contributed by low-energy photons, Mylar absorbers were placed between the targets and the x-ray detector. The energy resolution (full width at half maximum) of the x-ray detection system was 195 eV at 5.90 keV. The total efficiency and the energy calibration of the x-ray detection system were determined by placing standard calibrated x-ray sources of ^{51}Cr, ^{54}Mn, ^{57}Co, ^{65}Zn, ^{155}Eu, and ^{241}Am in the target position.

The ^{14}N ions elastically scattered from the targets were monitored simultaneously with the x-ray spectra by solid-state surface-barrier detectors mounted at the forward scattering angles of 30° and 45° with respect to the beam direction. The measured solid angles for the 30° and 45° detector were 3.0×10^{-3} sr and 8.0×10^{-4} sr, respectively. To determine if the elastic scattering was purely Rutherford, the particle yields for ^{14}N elastically scattered at 45° from Ge and 90° from an Au foil were simultaneously measured through the complete energy range from 7 to 35 MeV, and the ratio of the two yields was determined for each energy. The gold target was a self-supporting 100 $\mu g/cm^2$ foil placed 20 cm behind the Ge target. ^{14}N ions scattered from this foil were detected in a third surface-barrier detector subtending a solid angle of 7.4×10^{-4} sr. Within the experimental uncertainties due to counting statistics and target thickness, the measured ratio remained constant for all energies. Thus, it was assumed that the elastic scattering of ^{14}N from $_{32}Ge$ and all heavier elements was Rutherford.

Characteristic x-ray energies were determined from the centroids of the observed x-ray peaks and the energy calibration. Energy shifts were taken as the difference between the measured x-ray energies, and those for single K-shell ionization given by Bearden and Burr.[8] The amplified outputs from both x-ray and charged-particle detectors were recorded in 1000 channel sectors of a 16 000-channel analyzer consisting of a Tennecomp Pace/PDP 11/45 system and a CDC 3200 computer for plotting and data reduction by light-pen stripping. The dead time of the ADC determined the dead-time correction to the measured yields and was generally less than 10%. The count rates were sufficiently low that the detector dead time remained essentially zero.

III. DATA REDUCTION

The K-shell x-ray production cross section σ_x is given as

$$\sigma_x(E) = \frac{\Omega_R(\theta)}{Y_R(\theta)} \frac{d\sigma_R(E,\theta)}{d\Omega} \left(\frac{Y_{K\alpha}}{\epsilon_{K\alpha}} + \frac{Y_{K\beta}}{\epsilon_{K\beta}}\right) T , \qquad (1)$$

where $\Omega_R(\theta)$ is the measured solid angle subtended by the charged-particle detector at the laboratory scattering angle θ, $Y_R(\theta)$ is the total yield of Rutherford scattered particles at the angle θ corrected for background subtraction and dead time, $d\sigma_R(E,\theta)/d\Omega$ is the theoretical differential Rutherford scattering cross section for ions of energy E scattering at angle θ, $Y_{K\alpha,\beta}$ are the $K\alpha,\beta$ x-ray yields corrected for background and dead time, and $\epsilon_{K\alpha,\beta}$ are the absolute efficiencies of the x-ray detection system for the $K\alpha,\beta$ x rays. T, the thickness correction factor, is described by Laubert *et al.*[9] and includes approximate corrections to the x-ray and scattered-ion yields due to energy loss of the ions passing through targets of finite thickness. The maximum value of the thickness correction factor for this experiment was approximately 1.03. Equation (1) is based upon the assumption, verified by several authors,[10,11] that charged-particle-induced K x-ray emission is isotropic.

IV. RESULTS AND DISCUSSION

The measured values of the K x-ray production cross sections for the different energies and incident charge states of the ^{14}N ions are listed in Table I. The measured $K\alpha/K\beta$ intensity ratios and the $K\alpha$ and $K\beta$ energy shifts, ΔE_α and ΔE_β, are given in the same table. These results are discussed in the following sections.

A. K-shell x-ray production cross sections

The estimated absolute standard deviations for the measured x-ray production cross sections listed in Table I are approximately 10%. The method for determining these uncertainties has been discussed earlier.[6]

The experimental x-ray cross sections for representative targets of Ge, Zr, and Ag are plotted in Fig. 1 as a function of the incident ^{14}N ion energy and also as a function of the central para-

TABLE I. Experimental K-shell x-ray production cross sections, $K\alpha$ and $K\beta$ x-ray energy shifts and $K\alpha/K\beta$ x-ray intensity ratios from ^{14}N ion bombardment.[a]

Target element	E (MeV)	E/M (MeV/amu)	Incident charge state	σ_X (b)	$K\alpha/K\beta$	ΔE_α (eV)	ΔE_β (eV)
$_{32}$Ge	7.0	0.5	+3	1.97 ± 0.19		12 ± 10	76 ± 13
	8.4	0.6	+3	3.79 ± 0.35	6.76 ± 0.24	14 ± 8	96 ± 11
	9.8	0.7	+3	6.99 ± 0.66	6.62 ± 0.20	16 ± 7	106 ± 10
	12.6	0.9	+3	17.4 ± 1.6	6.33 ± 0.19	23 ± 7	125 ± 10
	15.4	1.1	+3	36.9 ± 3.4	6.29 ± 0.19	28 ± 7	133 ± 10
	18.2	1.3	+3	69.2 ± 6.6	6.21 ± 0.19	34 ± 7	143 ± 10
	21.0	1.5	+3	111 ± 10	5.81 ± 0.18	38 ± 7	155 ± 10
	23.8	1.7	+3	183 ± 18	5.62 ± 0.18	41 ± 7	165 ± 10
	26.6	1.9	+4	279 ± 27	5.56 ± 0.18	45 ± 7	168 ± 10
	29.4	2.1	+4	421 ± 41	5.52 ± 0.17	46 ± 7	169 ± 10
	32.2	2.3	+5	556 ± 56	5.49 ± 0.16	45 ± 7	170 ± 10
	36.0	2.57	+5	812 ± 80	5.43 ± 0.16	48 ± 7	168 ± 10
$_{37}$Rb	10.0	0.714	+3	1.97 ± 0.22	7.19 ± 1.34	0 ± 20	
	12.6	0.9	+4	4.74 ± 0.49	6.15 ± 0.77	8 ± 9	
	15.4	1.1	+4	9.61 ± 0.90	5.90 ± 0.24	15 ± 7	134 ± 15
	18.2	1.3	+4	17.6 ± 1.7	5.59 ± 0.25	18 ± 7	135 ± 15
	21.0	1.5	+4	30.8 ± 2.9	5.44 ± 0.22	21 ± 7	144 ± 15
	23.8	1.7	+4	44.4 ± 4.4	5.41 ± 0.21	24 ± 7	158 ± 10
	26.6	1.9	+4	69.1 ± 6.7	5.54 ± 0.22	28 ± 7	165 ± 10
	29.4	2.1	+4	96.2 ± 9.5	5.21 ± 0.21	30 ± 7	158 ± 10
	32.2	2.3	+5	138 ± 14	5.18 ± 0.16	33 ± 7	170 ± 10
	35.0	2.5	+5	182 ± 17	5.12 ± 0.18		
$_{39}$Y	15.4	1.1	+4	7.3 ± 0.77	5.77 ± 0.78		
	18.2	1.3	+4	12.8 ± 1.3	4.71 ± 0.31		
	21.0	1.5	+4	20.9 ± 2.1			
	23.8	1.7	+4	31.5 ± 3.3	5.51 ± 0.37		
	26.6	1.9	+4	47.0 ± 4.9	4.65 ± 0.24		
	32.2	2.3	+5	94.7 ± 9.8	4.89 ± 0.15	20 ± 6	167 ± 10
	35.0	2.5	+5	113 ± 10	4.79 ± 0.17		
$_{40}$Zr	15.4	1.1	+4	5.90 ± 0.65	4.74 ± 0.62	10 ± 10	
	18.2	1.3	+4	10.8 ± 1.1	5.07 ± 0.33	10 ± 9	188 ± 30
	21.0	1.5	+4	16.9 ± 1.7	4.73 ± 0.30	9 ± 9	124 ± 30
	23.8	1.7	+4	24.7 ± 2.5	4.83 ± 0.30	12 ± 10	
	26.6	1.9	+4	37.2 ± 3.9	4.64 ± 0.26	22 ± 8	139 ± 25
	29.4	2.1	+4	53.8 ± 5.3	4.76 ± 0.25	25 ± 14	166 ± 25
	32.2	2.3	+5	72.5 ± 7.8	4.74 ± 0.14	22 ± 7	166 ± 14
	35.0	2.5	+5	91.5 ± 8.6	4.80 ± 0.18		
$_{47}$Ag	12.6	0.9	+4	0.53 ± 0.07			
	15.4	1.1	+4	0.993 ± 0.093	4.82 ± 0.29	1 ± 10	128 ± 40
	18.2	1.3	+4	2.01 ± 0.19	4.86 ± 0.20	0 ± 8	124 ± 30
	21.0	1.5	+4	3.29 ± 0.31	4.73 ± 0.28	7 ± 10	148 ± 30
	23.8	1.7	+4	5.23 ± 0.49	4.81 ± 0.20		158 ± 30
	26.6	1.9	+4	7.15 ± 0.68	5.15 ± 0.31	15 ± 9	155 ± 30
	29.4	2.1	+4	10.6 ± 1.0	4.80 ± 0.24	12 ± 8	161 ± 25
	32.2	2.3	+5	14.7 ± 1.4	4.62 ± 0.17	15 ± 6	166 ± 17
	35.0	2.5	+5	20.3 ± 2.0	4.67 ± 0.19		

[a]All measured values are expressed with their estimated absolute standard deviations.

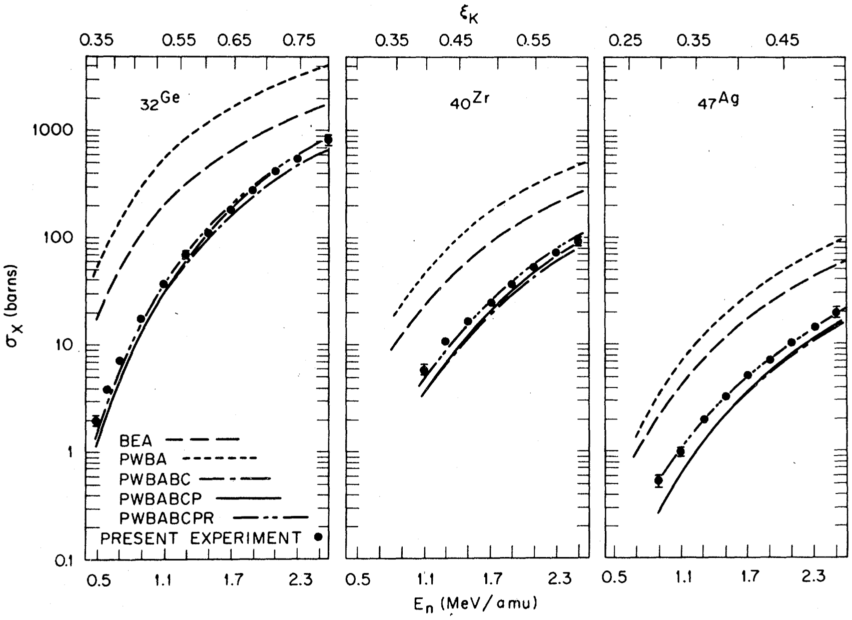

FIG. 1. Experimental ^{14}N ion-induced x-ray production cross sections compared to the binary-encounter approximation (BEA), the plane-wave Born approximation (PWBA), including binding energy and Coulomb deflection effects (PWBABC), also including polarization effects (PWBABCP), and an approximate relativistic correction (PWBABCPR). The parameter ξ_K is the ratio of the target-electron orbit time to the collision time.

eter ξ_K, which is the ratio of the characteristic orbital time of the K-shell electron to the time taken by the projectile to traverse the K-shell orbital. All of the measured cross sections are for values of ξ_K between 0.3 and 0.8.

The results of several theoretical calculations for K-shell ionization of the target elements by ^{14}N ion impact are also displayed in Fig. 1 where the ionization cross section σ_K is related to the x-ray production cross section σ_X through the relationship $\sigma_X = \omega_K \sigma_K$ where ω_K is the fluorescence yield. The values of ω_K used here are taken from the semiempirical "best values" determined by Bambynek *et al.*[12] They are 0.540 for Ge, 0.679 for Rb, 0.711 for Y, 0.730 for Zr, and 0.830 for Ag. These ω_K values were determined under the assumption that there were no vacancies in the L or M shells at the time of the K vacancy decay. In order to estimate the changes in the fluorescence yields due to multiple ionization, we have used a procedure of Larkins[13] to scale the radiative and Auger transition rates given by McGuire[14] by the fraction of the number of $2p$ electrons present in the L shell. We have made the assumption that the energy shifts observed are due entirely to $2p$ vacancies and have neglected $2s$, $3s$, and $3p$ vacancies. The number of $2p$ electrons present were estimated by comparing the measured $K\alpha$ and $K\beta$ energy shifts with those calculated from Hartree-Fock-Slater techniques.[15] We find an estimated maximum change in the fluorescence yield to be <6% for Ge and <2% for Ag.

The theoretical curves in Fig. 1 represent the predictions of the binary encounter approximation (BEA),[16-18] the plane-wave Born approximation (PWBA),[19,20] and the PWBA with the inclusion of the effects of increased target-electron binding energy and Coulomb deflection of the projectile by the target nucleus.[1,4] It is easily seen that the PWBA overpredicts the experimental cross sections by at least a factor of 5 for all targets, and the BEA overpredicts by a factor of 2 or more. The inclusion of the modifications for binding-energy and Coulomb-deflection effects in the PWBA bring the theoretical curves, labeled PWBABC, into much better agreement with the experimental values.

In order to account for the increase of the experimental cross sections over the corrected PWBA predictions for values of $\xi_K > 0.45$, Basbas *et al.*[4] have extended the formalism to include the effects of distortion of the target-electron wave function by the electromagnetic field of the incident particle. This is accomplished by modifying the incident-ion energy dependence of the binding-energy factor ϵ so that the magnitude of the cross section changes, but the universal behavior is preserved. In Fig. 1, the curves labeled PWBABCP show the results of the incorporation of this polarization effect.

At low incident-particle energies, the effect on the ionization cross sections of target electrons with relativistic velocities can be significant.[6,7,16,21,22] For the heavier K-shell elements such as Ag the relatively large energy transfers necessary for ionization by lower-energy ions

TABLE II. Approximate relativistic correction factors.

Target element	E_N (MeV)	$\frac{\sigma_{rel}}{\sigma_{nonrel}}$ (Hansen)	$\frac{\sigma_{rel}}{\sigma_{nonrel}}$ (Hönl)
$_{32}$Ge	7.0	1.32	1.17
	15.4	1.13	1.13
	36.0	1.05	1.11
$_{37}$Rb	10.0	1.40	1.18
	21.0	1.17	1.17
	35.0	1.09	1.15
$_{39}$Y	15.4	1.33	1.20
	23.8	1.19	1.19
	35.0	1.12	1.18
$_{40}$Zr	15.4	1.37	1.22
	23.8	1.22	1.20
	35.0	1.14	1.19
$_{47}$Ag	12.6	2.04	1.32
	32.2	1.30	1.31
	35.0	1.28	1.31

tends to increase the experimental cross sections. In order to obtain some quantitative estimate of this effect the energy-dependent correction factors calculated by Hansen[16] were employed. In Fig. 1, the curve labeled PWBABCPR is the result of applying the Hansen correction to the PWBA theory with polarization, binding-energy, and Coulomb-deflection effects included. Except for Ag, the theory with all corrections tends to slightly overestimate σ_X for values of $\xi_K > 0.55$ and underestimate σ_X for values of $\xi_K < 0.55$. For Ag, the relativistically corrected theory is in very good agreement with the experimental results.

An alternative relativistic correction method is that due to Hönl[22] as described by Merzbacher and Lewis.[19] It consists of modifying the screening parameter θ_K in the nonrelativistic PWBA formalism, and has the effect of raising the value of the calculated cross section. For all the elements studied the Hansen and Hönl corrections yielded the same value of the ionization cross section at $\xi_K \sim 0.5$. Above this point, the Hansen correction is the larger of the two, and below, the smaller of the two. Table II lists the values of the correction factors for representative nitrogen ion energies. Figures 1 and 2 display only the Hansen correction, since it appears to satisfy the proper energy dependence of the data.

Figure 2 shows the results of plotting scaled experimental x-ray production cross sections as a function of scaled projectile energy according to the prescription set forth by Basbas *et al.*,[1,4] where the factor ζ represents corrections to the screening parameter θ_K due to binding energy and polarization effects. The data are corrected from Coulomb deflection and relativistic target electron velocities by the factors $9E_{10}(\pi d q_0 \zeta)$ and $\sigma_{rel}/\sigma_{nonrel}$ (Hansen), respectively, to preserve the universality of the PWBA. Within experimental errors, the inclusion of Coulomb deflection, binding-energy increase, polarization, and relativistic effects to the PWBA provide good estimates of the data for these values. The modified PWBA appears to be quite valid for the projectile-target combinations and velocity range of the present experiment.

B. Energy shifts and $K\alpha/K\beta$ intensity ratios

The last three columns in Table I list the value of the $K\alpha/K\beta$ intensity ratios and the shifts in the characteristic $K\alpha$ and $K\beta$ x-ray energies as a function of ^{14}N ion energy. The primary contributions to the uncertainties are from the relative x-ray detector efficiencies (~2–3%), counting statistics, and centroid location. Figure 3 shows the results of plotting the ratio of $K\alpha/K\beta$ for ^{14}N ion bombardment to that for no multiple ionization as a function of the ratio of the velocity of the ^{14}N ion (V_1) to the average velocity of L-shell electron (V_L), the ratio being given by $V_1/V_L = (E/\lambda \bar{U}_L)^{1/2}$. E is the ^{14}N ion energy, λ is the ratio of ^{14}N mass to the electron mass, and $\bar{U}_L$ is the weighted-average L-shell binding energy $[\bar{U}_L = \frac{1}{4}(U_{L_1} + U_{L_2} + 2U_{L_3})]$.

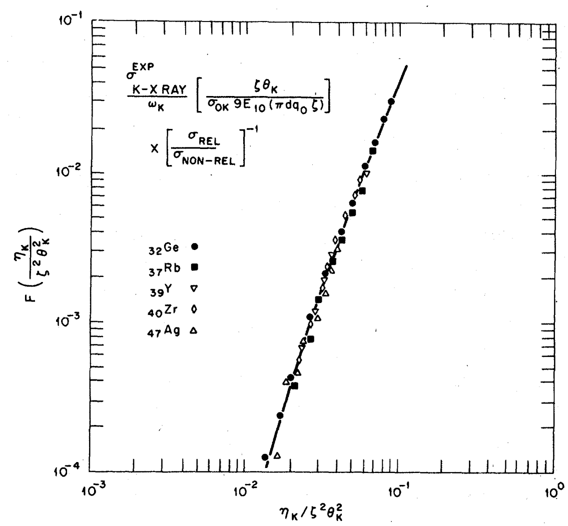

FIG. 2. Scaled experimental x-ray production cross section for ^{14}N ion impact as a function of scaled energy for comparison with the universal function $F(\eta_K/\zeta^2\theta_K^2)$ as defined by Basbas *et al.* in Refs 1 and 4. The data have been corrected for Coulomb deflection and relativistic effects (Hansen, Ref. 16) and the screening parameter θ_K has been corrected to reflect increased binding energy and polarization through the factor ζ.

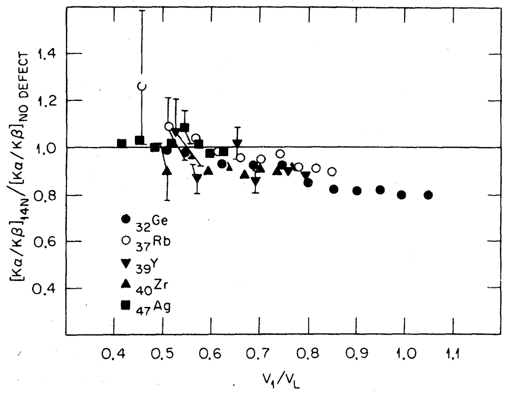

FIG. 3. Ratio of $K\alpha/K\beta$ for ^{14}N ion bombardment divided by the same ratio with no multiple ionization, as a function of the relative velocity between the ^{14}N ion and an average L-shell electron.

The $K\alpha/K\beta$ values for no multiple ionization are those of Salem *et al.*[23]; they are 6.8 for Ge, 5.68 for Rb, 5.41 for Y, 5.26 for Zr, and 4.73 for Ag. Figure 4 shows the energy shifts of the $K\alpha$ and $K\beta$ x-ray groups and their estimated standard deviations for Ge as a function of the incident ^{14}N ion energy, and as functions of V_1/V_L and V_1/V_M, the velocity ratios for the L and M shells.

The magnitudes of the energy shifts and the deviation of the $K\alpha/K\beta$ ratios from the zero-defect configuration values contain information about the amounts of L and M shell vacancy production that occur simultaneously with K vacancy production. It has been demonstrated that the fraction of K x rays produced in the presence of n L vacancies may be approximated by the nth term of a binomial series which has been interpreted within the BEA formalism.[16,24-27] In order to develop some quantitative idea about the amount of multiple ionization occurring during ^{14}N ion bombardment, the BEA prescription for multiple ionization was applied to the case of Ge.

At 7 MeV the calculated percentage of K x rays emitted with zero, one, two and three L-shell vacancies is 61%, 31%, 7%, and 1%, respectively. At 36 MeV these percentages change to 20%, 36%, 28%, and 13%, or an average of approximately one L-shell vacancy. Based upon Hartree-Fock-Slater (HFS) calculations[15] of atomic energy levels for different defect configurations, the calculated $K\alpha$ and $K\beta$ energy shifts are approximately 42 and 90 eV, respectively, per $2p$ vacancy and an average of approximately 0 and 5 eV, respectively, per M-shell vacancy. Using the calculated percentages above and assuming no significant change in M-shell occupancy, this would indicate $K\alpha$ and $K\beta$ shifts of 20 and 40 eV, respectively, at 7 MeV, and 60 and 120 eV, respectively, at 35 MeV.

These calculations are consistent with the energy-shift data for Ge and indicate the probable dominance of L-shell ionization in producing energy shifts and changes in $K\alpha/K\beta$ ratios. Such dominance is consistent with the peaking of the Ge energy shifts at 36 MeV, which corresponds to $V_1/V_L \cong 1$, or the energy at which maximum L-shell ionization takes place according to both BEA and PWBA theories. Similar analyses may be applied to the other elements with results supporting the arguments made above.

For moderate amounts of L-shell multiple ionization the K-shell fluorescence yields and the $K\alpha/K\beta$ intensity ratios may be approximated by using the procedure described by Larkins[13] and recently applied to ^{12}C ion bombardment of $_{22}$Ti by Watson and Li.[28] This procedure scales the $K\alpha/K\beta$ ratio for the zero-defect configuration by the relative populations of the $2p$ and $3p$ subshells in a particular defect configuration in order

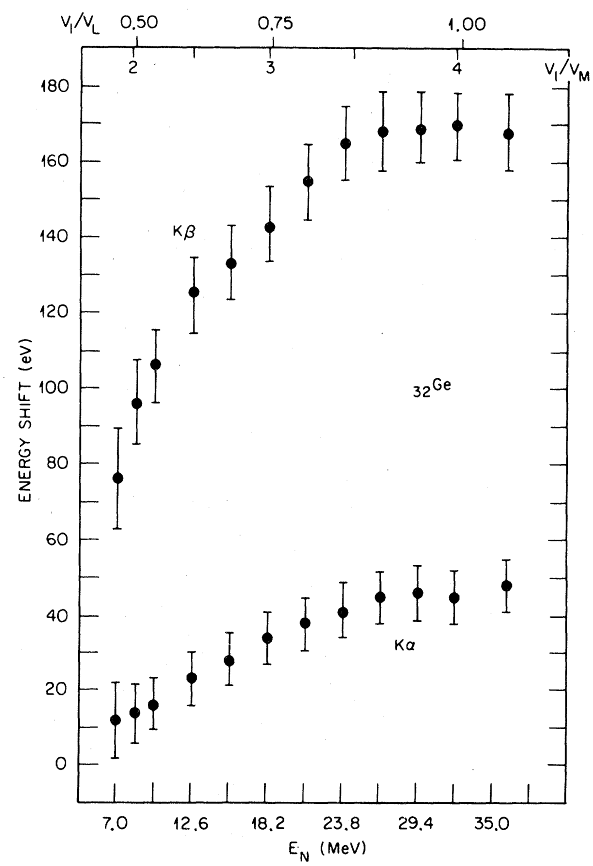

FIG. 4. Energy shifts of the $K\alpha$ and $K\beta$ x-ray groups of Ge produced by ^{14}N ion impact as a function of the energy of the incident ^{14}N ion. V_1/V_L and V_1/V_M are the ratios of the relative velocities between the ^{14}N ion and average L-shell and M-shell electrons, respectively.

to obtain the $K\alpha/K\beta$ ratio for that configuration. The results in Fig. 3 indicate that, for cases of moderate multiple ionization, the average relative populations of the $2p$ and $3p$ levels of all the targets are approximately equal for equal values of V_1/V_L between 0.5 and 1.

The values of the K-shell fluorescence yields for small amounts of L-shell multiple ionization were shown above not to be significantly different from the values for no multiple ionization. This has also been verified experimentally by Moore and Mathews[29] for neon targets.

V. SUMMARY

The PWBA theory modified to include the effects of increased target binding energy, Coulomb deflection of the incident ion, polarization of the target by the field of the impinging ion, and the relativistic velocities of target electrons gives good estimates of the experimentally measured x-ray production cross sections produced by ^{14}N ion bombardment of target elements of $32 \leq Z \leq 47$ for energies between 7–35 MeV. The measured x-ray production cross sections also display an approximate universal behavior which is predicted by the modified PWBA. A rigorous incorporation of the relativistic effects into the PWBA formalism could do much toward developing a comprehensive model of ion-indiced vacancy production.

The measured $K\alpha$ and $K\beta$ energy shifts and intensity ratios indicate that the most probable number of L vacancies created simultaneously with a K vacancy is 1 or less for all the targets, and the L vacancy production dominates the changes in the energy shifts and intensity ratios. The behavior of the $K\alpha/K\beta$ ratios with increasing V_1/V_L (the ion velocity divided by the L electron velocity) indicates that, for values of V_1/V_L between 0.5 and 1.0, the average relative population of the $2p$ and $3p$ subshells is the same for all target elements.

Measurements of x-ray production cross sections, intensity ratios and energy shifts for lower and higher energies than those of this work would be useful in determining the limits of validity of the PWBA theory.

ACKNOWLEDGMENTS

The authors would like to express their sincere appreciation to F. Elliott, R. K. Rice, R. Mehta, and A. D. Ray for their assistance with the data acquisition and analysis. Special thanks go to G. D. Alton, E. Richardson, W. T. Milner, J. A. Biggerstaff, C. D. Moak, N. F. Ziegler, and R. P. Cumby of the staff of the Oak Ridge National Laboratory for their invaluable aid with the operation and maintenance of the experimental facilities of the tandem Van de Graaff laboratory. The authors are indebted to G. Basbas and R. Laubert for providing the theoretical calculations of their modified PWBA.

---

*These experiments were performed at the Oak Ridge National Laboratory Tandem Van de Graaff Facility which is supported by ERDA and operated by Union Carbide Corp. Travel for participants was provided by the Oak Ridge Associated Universities through contractual arrangement with ERDA.

†Supported by The Robert A. Welch Foundation, the NTSU Faculty Research Fund, and The Research Corp.

[1]G. Basbas, W. Brandt, and R. Laubert, Phys. Rev. A 7, 983 (1973).

[2]G. Bissinger, P. H. Nettles, S. M. Shafroth, and A. W. Waltner, Phys. Rev. A 10, 1932 (1974).

[3]R. M. Wheeler, R. P. Chaturvedi, J. L. Duggan, J. Tricomi, and P. D. Miller, Phys. Rev. A 13, 958 (1976).

[4]G. Basbas, W. Brandt, and R. Laubert (private communication).

[5]T. L. Hardt and R. L. Watson, Phys. Rev. A 7, 1917 (1973).

[6]F. D. McDaniel, T. J. Gray, R. K. Gardner, G. M. Light, J. L. Duggan, H. A. van Rinsvelt, R. D. Lear, G. H. Pepper, J. W. Nelson, and A. R. Zander, Phys. Rev. A 12, 1271 (1975).

[7]D. Jamnik and C. Zupancic, Mat. Fys. Medd. Dan. Vid. Selsk. 31, No. 2 (1957).

[8]J. A. Bearden and A. F. Burr, Rev. Mod. Phys. 39, 78 (1967).

[9]R. Laubert, H. Haselton, J. R. Mowat, R. S. Peterson, and I. A. Sellin, Phys. Rev. A 11, 135 (1975).

[10]L. M. Middleman, R. L. Ford, and R. Hofstadter, Phys. Rev. A 2, 1429 (1970).

[11]E. H. Pedersen, S. J. Czuchlewski, M. D. Brown, L. D. Ellsworth, and J. R. Macdonald, Phys. Rev. A 11, 1267 (1975).

[12]W. Bambynek, B. Crasemann, R. W. Fink, H.-U. Freund, H. Mark, C. D. Swift, R. E. Price, and P. V. Rao, Rev. Mod. Phys. 44, 716 (1972).

[13]F. P. Larkins, J. Phys. B 4, L29 (1971).

[14]E. J. McGuire, Phys. Rev. A 2, 273 (1970).

[15]F. Herman and S. Skillman, *Atomic Structure Calculations* (Prentice-Hall, Englewood Cliffs, N.J., 1963).

[16]J. S. Hansen, Phys. Rev. A 8, 822 (1973).

[17]J. H. McGuire and P. Richard, Phys. Rev. A 8, 1374 (1973).

[18]J. H. McGuire and K. Omidvar, Phys. Rev. A 10, 182 (1974).

[19]E. Merzbacher and H. Lewis, *Encyclopedia of Physics*, edited by S. Flugge (Springer-Verlag, Berlin, 1958), Vol. 34, p. 166.

[20]G. S. Khandelwal, B.-H. Choi, and E. Merzbacher, At. Data 1, 103 (1969).

[21]B.-H. Choi, Phys. Rev. A 4, 1002 (1971).

[22]H. Hönl, Z. Phys. 84, 1 (1933).

[23]S. I. Salem, S. L. Panossian, and R. A. Krause, At.

Data Nucl. Data Tables 14, 91 (1974).
[24]D. Burch and H. Swanson, in *Proceedings of the International Conference on Inner Shell Ionization Phenomena and Future Applications,* CONF-720404 (National Technical Information Service, Springfield, Va., 1973), p. 1464.
[25]R. L. Kauffman, J. H. McGuire, P. Richard, and C. F. Moore, Phys. Rev. A 8, 1233 (1973).
[26]R. L. Kauffman, C. W. Woods, K. A. Jamison, and P. Richard, Phys. Rev. A 11, 872 (1975).
[27]J. H. McGuire, Phys. Rev. A 9, 286 (1974).
[28]R. L. Watson and T. K. Li, Phys. Rev. A 4, 132 (1971); 9, 1574 (1974).
[29]C. F. Moore and D. L. Matthews, *Proceedings of the Third Conference on Application of Small Accelerators, Denton, Texas, 1974,* edited by J. L. Duggan and I. L. Morgan, CONF-741040 (National Technical Information Service, Springfield, Va., 1974), Vol. I, p. 419.